Volume 48
Number 2
14 January 2024
Pages 421–992

NJC

New Journal of Chemistry

A journal for new directions in chemistry

rsc.li/njc

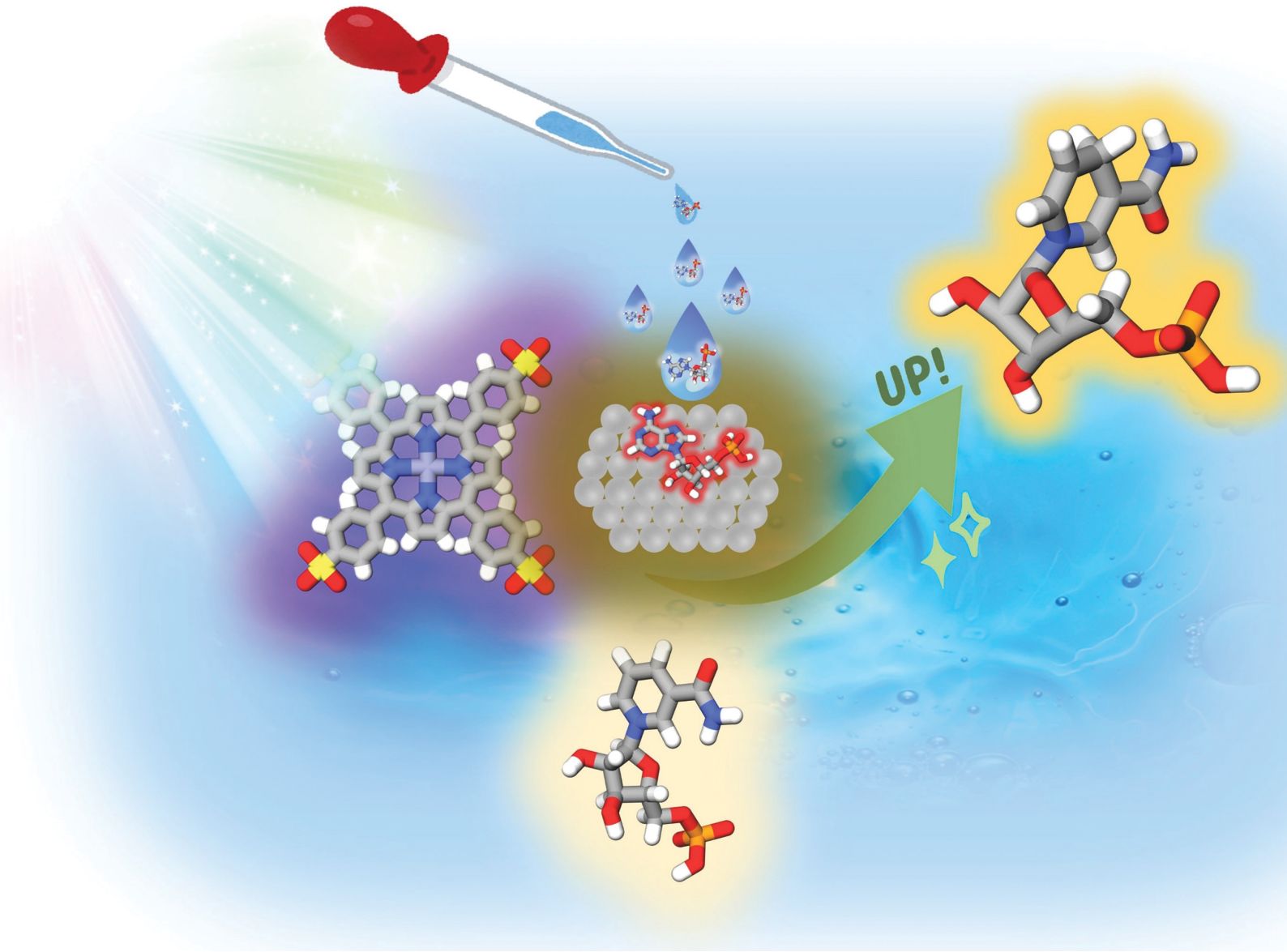

ISSN 1144-0546

COMMUNICATION

Kazuma Suehiro and Yutaka Amao

Effect of adenosine monophosphate on visible-light driven nicotinamide mononucleotide reduction in a system of water-soluble zinc porphyrin and colloidal rhodium nanoparticles

ROYAL SOCIETY OF CHEMISTRY

cnrs

NJC

ROYAL SOCIETY OF CHEMISTRY

COMMUNICATION

View Article Online
View Journal | View Issue

Cite this: *New J. Chem.*, 2024, **48**, 506

Received 20th October 2023,
Accepted 14th November 2023

DOI: 10.1039/d3nj04875f

rsc.li/njc

Effect of adenosine monophosphate on visible-light driven nicotinamide mononucleotide reduction in a system of water-soluble zinc porphyrin and colloidal rhodium nanoparticles†

Kazuma Suehiro[a] and Yutaka Amao *[ab]

NAD$^+$ analogues, nicotinamide and nicotinamide mononucleotide (NMN$^+$), were used to clarify the mechanism of visible-light driven selective NAD$^+$ reduction to 1,4-NADH in a system of water soluble zinc tetraphenylporphyrin tetrasulfonate and colloidal rhodium nanoparticles dispersed with polyvinylpyrrolidone (Rh-PVP). As a result, it was found that nicotinamide was not reduced but NMN$^+$ was reduced to the 1,4-form selectivity, the same as NAD$^+$. In addition, the visible-light driven selective NMN$^+$ reduction was found to be enhanced by the addition of the adenosine monophosphate part of the NAD$^+$ structure.

The reduced form of nicotinamide adenine dinucleotide (NADH) and nicotinamide adenine dinucleotide (NAD$^+$) are widely used as co-enzymes with electron donor and electron acceptor functions, respectively, in redox reactions with oxidoreductase.[1–3] Due to the high cost and low stability of NADH, its supply is a major challenge and the development of effective NADH regeneration systems is being actively pursued.[4,5] Various NADH regeneration methods have been investigated using chemical processes,[6,7] biocatalysis,[8] electrochemistry,[9,10] photochemistry,[11,12] and homogeneous[13] and heterogeneous catalysis.[14] Of these methods, photochemical NADH regeneration has attracted much attention, because solar energy is clean, cheap, abundant, and renewable. The direct reduction of NAD$^+$ to NADH using photosensitisers such as water-soluble metalloporphyrins with absorption bands in the visible light region has been proposed as a simple method for reducing NAD$^+$ to NADH using visible light energy. NAD$^+$ is reduced in a single-electron process by a photosensitiser to form an NAD radical, and then undergoes dimerisation to form a biologically inactive reduction product, as shown in Fig. 1.[15] In addition, it has been reported that enzymatically inactive by-products (1,2- and 1,6-NADH isomers) also are produced, as shown in Fig. 1.

Therefore, systems that selectively reduce NAD$^+$ to 1,4-NADH require effective catalysts that prevent NAD$^+$ dimerisation and 1,2- or 1,6-NADH isomer production. As examples of catalysts for the reduction of NAD$^+$ to 1,4-NADH, organometallic complexes have been reported using ruthenium, rhodium, and iridium ions. In particular, the rhodium complex $[Cp^*Rh(bpy)(H_2O)]^{2+}$ (Cp^* = pentamethylcyclopentadienyl, bpy = 2,2′-bipyridyl) has been widely used and studied for the

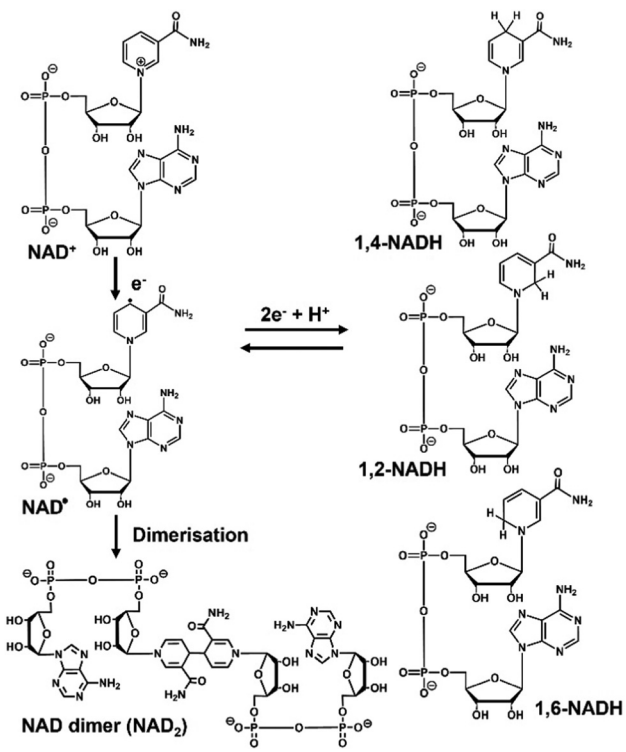

Fig. 1 Schematic representation of a typical NAD$^+$ reduction pathway.

[a] *Graduate School of Science, Osaka Metropolitan University, 3-3-138 Sugimoto, Sumiyoshi-ku, Osaka 558-8585, Japan*
[b] *Research Centre for Artificial Photosynthesis (ReCAP), Osaka Metropolitan University, 3-3-138 Sugimoto, Sumiyoshi-ku, Osaka 558-8585, Japan. E-mail: amao@omu.ac.jp*

† Electronic supplementary information (ESI) available: Experimental section, additional data. See DOI: https://doi.org/10.1039/d3nj04875f

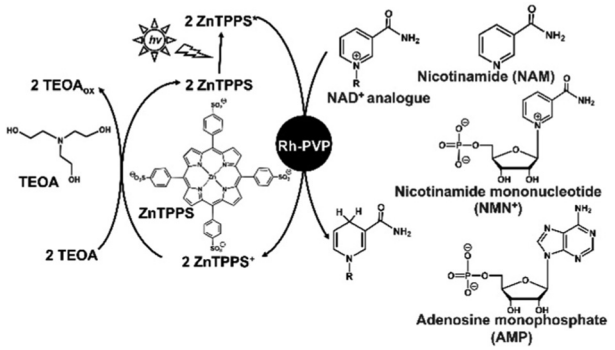

Fig. 2 Visible-light driven 1,4-NADH regeneration in a system of TEOA, ZnTPPS, and Rh-PVP. The chemical structures of nicotinamide (NAM), nicotinamide mononucleotide (NMN^+) and adenosine monophosphate (AMP) are shown.

regioselective reduction of NAD^+ because of its versatile range of application and regioselective activity.[16,17] As an example of the non-enzymatic photoreduction of NAD^+, $[Cp^*Rh(bpy)(H_2O)]^{2+}$ has also been used as a catalyst for electron and hydride transfer in the presence of a photosensitizer.[18,19] Thus, we focused on Rh catalysts because of their usefulness in hydride production. One type of Rh catalyst, colloidal Rh nanoparticles dispersed by protective agents such as polymers and surfactants, has attracted considerable attention due to its simple preparation method by the reduction of Rh^{3+} ions in ethanol solvent with protective agents. In particular, Rh nanoparticles dispersed in polyvinylpyrrolidone (Rh-PVP) have attracted significant attention due to their ability to catalyse the hydrogenation of benzoic acids and nitriles. A visible-light driven regioselective 1,4-NADH regeneration system consisting of triethanolamine (TEOA) as an electron donor, zinc tetraphenylporphyrin tetrasulfonate (ZnTPPS) as a photosensitizer, and Rh-PVP as a selective NAD^+ reduction catalyst, as shown in Fig. 2, has been reported.[20,21]

By using this system, NAD^+ is selectively reduced to enzymatically active 1,4-NADH upon visible-light irradiation. Moreover, in this system, it has been found that NAD^+ can be selectively reduced to 1,4-NADH using TiO_2 photocatalyst as a sensitiser in addition to ZnTPPS.[21] However, a detailed 1,4-NADH regeneration mechanism with Rh-PVP in this system has not been clarified yet. One way to clarify this mechanism is to study the interaction of Rh-PVP with each of the NAD^+ components, nicotinamide, pyrophosphate, adenine and pentose, as shown in Fig. 2.

In this study, focusing on the unique catalytic function of Rh-PVP, we attempted the selective photoreduction of NAD^+ to enzyme active 1,4-NADH by using Rh-PVP in a photo-redox system, without producing by-products, based on the effect of each of the NAD^+ components, nicotinamide, pyrophosphate, adenine and pentose. Here, we report a novel and simple system using homogeneous polymer-dispersed Rh nanoparticles for selective 1,4-NADH regeneration.

First, the visible-light driven reduction of NAD^+ analogues, NAM, NAD^+ and NMN^+, in a system of TEOA, ZnTPPS and Rh-PVP was compared. ZnTPPS was purchased from Frontier Scientific,

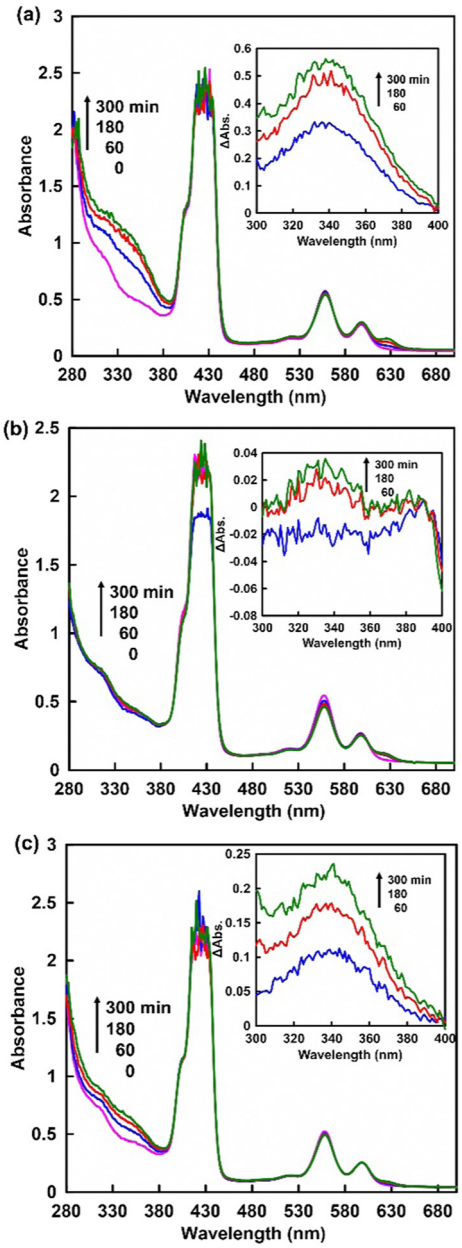

Fig. 3 UV-vis absorption spectra changes in the sample solution consisting of TEOA, ZnTPPS, Rh-PVP and NAD^+ analogues with irradiation. (a) NAD^+, (b) NAM, (c) NMN^+. Inset: Different UV-Vis absorption spectra of the sample solution from 0 min irradiation.

Inc. Rh-PVP was purchased from Renaissance Energy Research. NAD^+ was purchased from Oriental Yeast Co., Ltd. NAM and NMN^+ were purchased from Tokyo Chemical Industry Co., Ltd. The reduction of NAD^+ analogues using a system containing TEOA (0.2 M), ZnTPPS (4.6 μM), Rh-PVP (Rh concentration: 50 μM) and NAD^+ analogues (1.0 mM) was investigated in 5.0 mL of 50 mM HEPES-NaOH buffer (pH 7.4) at 30 °C. A sample solution was deaerated by freeze–pump–thaw cycling, and flushed with Ar gas for 10 min. Then, the sample solution was irradiated with a halogen lamp as a visible-light energy source. The production of a reduced NAD^+ analogue was

determined based on the UV-Vis absorption change at 340 nm. Fig. 3 shows the time dependence of UV-vis absorption spectra changes in the sample solution consisting of TEOA, ZnTPPS, Rh-PVP and NAD^+ analogues with irradiation. Different UV-Vis absorption spectra changes of the sample solution from 0 min irradiation are shown in the inset of Fig. 3.

When using NAD^+ or NMN^+, the intensity of the absorption band with a maximum at 340 nm was increased as shown in Fig. 3(a) and (c). In contrast, no significant change in the absorption band with a maximum at 340 nm was observed when using NAM as an NAD^+ analogue, as shown in Fig. 3(b). These results indicate that NMN^+ was reduced to NMNH, while no reduction of NAM occurred when using the system of TEOA, ZnTPPS and Rh-PVP with visible-light irradiation. This suggests that quaternization of the pyridine nitrogen of nicotinamide is essential for selective reduction using a system of TEOA, ZnTPPS and Rh-PVP with visible-light irradiation. For NMN^+ reduction, absorption maxima at 395 nm, based on 1,2-NMNH, and 345 nm, based on 1,6-NMNH, were not observed, as shown in Fig. 3(c). This indicated that NMN^+ was reduced to 1,4-NMNH or NMN dimer. Therefore, isomer analysis of the reduction products of NMN^+ was conducted by using an HPLC system with a TOSHO ODS column (4.6 × 250 mm, 5 μm particle size), a Shimadzu LC-20AD SP pump, and a Shimadzu SPD-20A UV/Vis detector (detected wavelength; 340 nm). A mixed solution of methanol/100 mM potassium phosphate buffer pH 7.1 (9 : 1 v/v) was used as the eluent. Fig. 4 shows the analytical HPLC chromatograms for visible-light driven NMN^+ reduction with the system consisting of TEOA, ZnTPPS, Rh-PVP and NMN^+ (a), and a standard sample of ((2*R*,3*S*,4*R*,5*R*)-5-(3-carbamoylpyridin-1(4*H*)-yl)-3,4-dihydroxy-tetrahydrofuran-2-yl)methyl dihydrogen phosphate (1,4-NMNH) purchased from AmBeed, Inc (b).

As shown Fig. 4(a), the intensity of the signal peak based on 1,4-NMNH increased with irradiation time. Thus, NMN^+ was reduced to 1,4-NMNH only using the visible-light redox system of TEOA, ZnTPPS and Rh-PVP.

Next, we discuss the quantification of the visible-light reduction of NMN^+ to 1,4-NMNH using the visible-light redox system of TEOA, ZnTPPS and Rh-PVP. The production of 1,4-NMNH was determined based on the UV-Vis absorption change at 340 nm with a molar extinction coefficient of 0.884 mM^{-1} cm^{-1} (Fig. S1 (ESI†) shows the UV-Vis absorption spectra of various 1,4-NMNH concentrations, and the relationship between 1,4-NMNH concentration and the absorbance at 340 nm). Fig. 3 shows the time dependence of the UV-Vis absorption spectra changes in the sample solutions consisting of TEOA, ZnTPPS, Rh-PVP and NAD^+ analogues (NMN^+ (a) or NAD^+ (c)) with irradiation. Fig. 5 shows the time dependence of 1,4-NMNH and 1,4-NADH production using the system of TEOA, ZnTPPS, Rh-PVP and NMN^+ or NAD^+ with irradiation.

As shown in Fig. 5, the concentrations of 1,4-NMNH and 1,4-NADH increased with increasing irradiation time. After 300 min of irradiation, the concentrations of 1,4-NMNH and 1,4-NADH were estimated to be 249 and 61.1 μM, respectively. The yields for 1,4-NMNH and 1,4-NADH production were calculated to be 24.9 and 6.1%, respectively. These results suggest that the visible-light reduction efficiency is related to the AMP moiety, which is the difference in structure between NAD^+ and NMN^+.

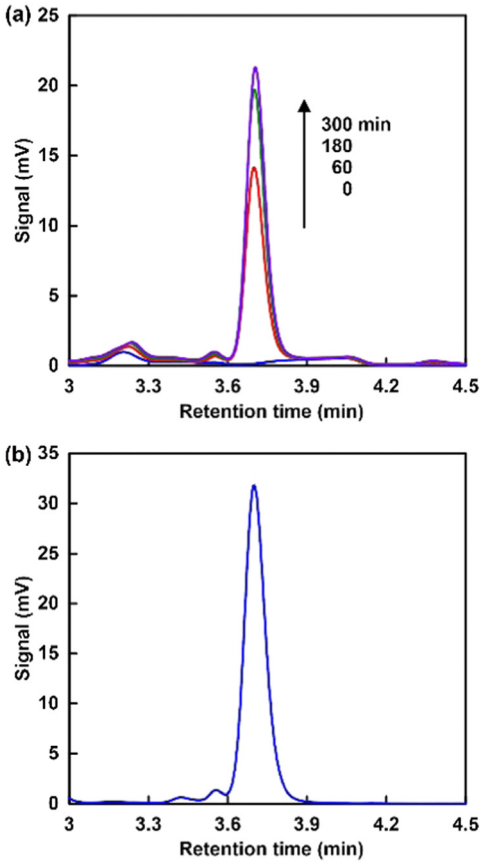

Fig. 4 HPLC chromatograms for visible-light driven NMN^+ reduction with the system consisting of TEOA, ZnTPPS, Rh-PVP and NMN^+ with different irradiation times (a), and a standard sample of 1,4-NMNH (b).

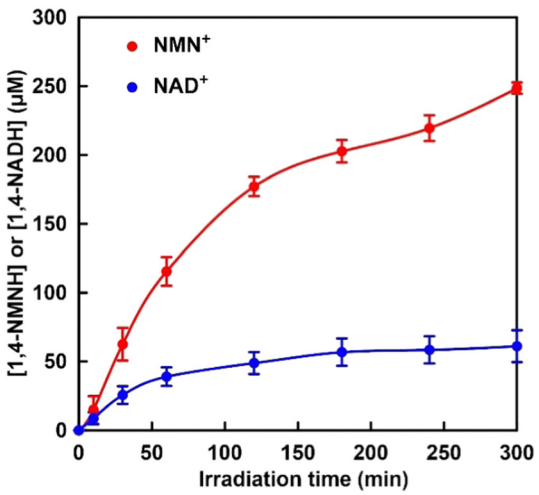

Fig. 5 Time dependence of 1,4-NMNH (red) and 1,4-NADH (blue) production with the system of TEOA, ZnTPPS, Rh-PVP and nicotinamide analogue (NMN^+ or NAD^+) with irradiation.

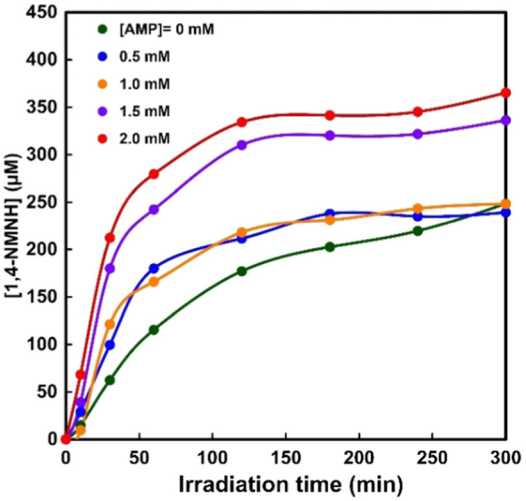

Fig. 6 Time dependence of 1,4-NMNH production with the system of TEOA, ZnTPPS, Rh-PVP and NMN^+ with irradiation in the presence of various AMP concentrations.

In order to investigate the effect of the AMP moiety on NAD^+ reduction to 1,4-NADH, a sample solution containing TEOA (0.2 M), ZnTPPS (25 μM), Rh-PVP (Rh concentration: 50 μM), NMN^+ (1.0 mM), and AMP (0–2.0 mM) was irradiated with visible-light, the same as for the previous experiment. Fig. S2 (ESI†) shows the time dependence of the UV-Vis absorption spectra changes in the sample solution consisting of TEOA, ZnTPPS, Rh-PVP and NMN^+ with irradiation in the presence of AMP (0–2.0 mM). Fig. 6 shows the time dependence of 1,4-NMNH production using the system of TEOA, ZnTPPS, Rh-PVP and NMN^+ with irradiation at various AMP concentrations. As shown in Fig. 6, the concentration of 1,4-NMNH increased with increasing irradiation time at all AMP concentrations. Under conditions with less than 1.0 mM AMP, the initial rate of 1,4-NMNH production increased, but the concentration of 1,4-NMNH produced after 5 h of irradiation was almost the same as that in the absence of AMP. On the other hand, the initial rate of 1,4-NMNH production increased with more than 1.5 mM AMP, and the concentration of 1,4-NMNH produced after 5 h of irradiation was found to increase by about fourfold compared to the system in the absence of AMP.

From these results, it was found that the visible-light reduction efficiency of NMN^+ to 1,4-NMNH was increased up to 1.4-fold by adding more than 1.5 equivalents of AMP to the NMN^+ concentration. No change in the visible-light reduction efficiency of NMN^+ to 1,4-NMNH was observed in the presence of adenosine. In contrast, no change in the efficiency of the visible light driven NAD^+ reduction to 1,4-NADH was observed in the presence of AMP. This suggests that the pyrophosphate and adenosine moieties constituting NAD^+ play an important role in Rh-PVP-catalysed 1,4-NADH generation.

In this work, to elucidate the mechanism of visible light-driven selective NAD^+ reduction to 1,4-NADH in the system of ZnTPPS and Rh-PVP, the visible light reduction behaviour of the NAD^+ analogues NAM and NMN^+ was investigated. As a result, no reduction of nicotinamide was observed, but NMN^+ was reduced to the 1,4-form selectivity. It was found that the quaternisation of the pyridine nitrogen of nicotinamide is essential for selective reduction upon visible light irradiation using TEOA, ZnTPPS and Rh-PVP. In addition, it was found that the visible-light driven selective NMN^+ reduction to 1,4-NMNH was enhanced by the addition of the adenosine monophosphate part of the NAD^+ structure. This work provides a platform for using colloidal Rh nanoparticles as highly efficient homogeneous catalysts for 1,4-NADH regeneration.

Conflicts of interest

There are no conflicts to declare.

Acknowledgements

This work was partially supported by Grant-in-Aid for Specially promoted Research (23H05404), Scientific Research (B) (22H 01872), (22H01871) and Fund for the Promotion of Joint International Research (Fostering Joint International Research (B)) (19KK0144), and by Institute for Fermentation, Osaka (IFO) (G-2023-3-050).

Notes and references

1 A. T. Martínez, F. J. Ruiz-Dueñas, S. Camarero, A. Serrano, D. Linde, H. Lund, J. Vind., M. Tovborg, O. M. Herold-Majumdar, M. Hofrichter, C. Liers, R. Ullrich, K. Scheibner, G. Sannia, A. Piscitelli, C. Pezzella, M. E. Sener, S. Kılıç, W. J. H. van Berkel., V. Guallar, M. F. Lucas, R. Zuhse, R. Ludwig, F. Hollmann, E. Fernández-Fueyo, E. Record, C. B. Faulds, M. Tortajada, I. Winckelmann, J.-A. Rasmussen., M. Gelo-Pujic, A. Gutiérrez, J. C. del Río, J. Rencoret and M. Alcalde, *Biotechnol. Adv.*, 2017, **35**, 815.
2 L. S. Vidal, C. L. Kelly, P. M. Mordaka and J. T. Heap, *Biochim. Biophys. Acta, Proteins Proteomics*, 2018, **1866**, 327.
3 J. K. B. Cahn, C. A. Werlang, A. Baumschlager, S. Brinkmann-Chen, S. L. Mayo and F. H. Arnold, *ACS Synth. Biol.*, 2017, **6**, 326.
4 X. Wang, T. Saba, H. H. P. Yiu, R. F. Howe, J. A. Anderson and J. Shi, *Chemistry*, 2017, **2**, 621.
5 H. Wu, C. Tian, X. Song, C. Liu, D. Yanga and Z. Jiang, *Green Chem.*, 2013, **15**, 1773.
6 K. E. Taylor and J. B. Jones, *J. Am. Chem. Soc.*, 1976, **98**, 5689.
7 A. Dibenedetto, P. Stufano, W. Macyk, T. Baran, C. Fragale, M. Costa and M. Aresta, *ChemSusChem*, 2012, **5**, 373.
8 D. Mandler and I. Willner, *J. Am. Chem. Soc.*, 1984, **106**, 5352.
9 S. Immanuel, R. Sivasubramanian, R. Gul and M. A. Dar, *Chem. – Asian J.*, 2020, **15**, 4256.
10 C. S. Morrison, W. B. Armiger, D. R. Dodds, J. S. Dordick and M. A. G. Koffas, *Biotechnol. Adv.*, 2018, **36**, 120.
11 D. Yang, H. Zou, Y. Wu, J. Shi, S. Zhang, X. Wang, P. Han, Z. Tong and Z. Jiang, *Ind. Eng. Chem. Res.*, 2017, **56**, 6247.

12 A. Sánchez-Iglesias, J. Barroso, D. M. Solís, J. M. Taboada, F. Obelleiro, V. Pavlov, A. Chuvilin and M. Grzelczak, *J. Mater. Chem. A*, 2016, **4**, 7045.
13 S. Fukuzumi, Y.-M. Lee and W. Nam, *J. Inorg. Biochem.*, 2019, **199**, 110777.
14 X. Wang and H. H. P. Yiu, *ACS Catal.*, 2016, **6**, 1880.
15 T. Saba, J. Li, J. W. H. Burnett, R. F. Howe, P. N. Kechagiopoulos and X. Wang, *ACS Catal.*, 2021, **11**, 283.
16 E. Steckhan, S. Herrmann, R. Ruppert, J. Thömmes and C. Wandrey, *Angew. Chem., Int. Ed. Engl.*, 1990, **29**, 388.
17 H. C. Lo, O. Buriez, J. B. Kerr and R. H. Fish, *Angew. Chem., Int. Ed.*, 1999, **38**, 1429.
18 J. Canivet, G. Süss-Fink and P. Štěpnička, *Eur. J. Inorg. Chem.*, 2007, 4736.
19 F. Hildebrand, C. Kohlmann, A. Franz and S. Lütz, *Adv. Synth. Catal.*, 2008, **350**, 909.
20 T. Katagiri and Y. Amao, *New J. Chem.*, 2021, **45**, 15748.
21 T. Katagiri and Y. Amao, *Sustainable Energy Fuels*, 2022, **6**, 2581.

